13th World Conference on Earthquake Engineering
Vancouver, B.C., Canada
August 1-6, 2004
Paper No. 2553

THEORETICAL EVALUATION OF ATTENUATION RELATIONSHIP IN DISTANCE FOR GROUND MOTION

Hiroshi DOHI[1], Masahiro KAWANO[2], Koichiro ASANO[3], and Satoshi MATSUDA[4]

SUMMARY

In this paper, to examine more precisely prediction potential of the ground motion model on the basis of wave propagation theory and source kinematics, first the decay of seismic wave with propagation distance has been evaluated using the ground motion model. Second such seismic wave attenuation has been compared with the ones for the ground motions observed at several sites. The research into seismic wave attenuation has suggested that the source-site distance, the source-site geometry, particularly the ratio of epicentral distance to focal depth, and the directivity effects in the source radiation are related essentially to the description of attenuation of ground motion.

INTRODUCTION

In the previous paper[1)], the prediction model of ground motion has been presented on the basis of wave propagation theory and source kinematics. In this modeling of ground motion, the rupture process for a unit event on the fault plane has been idealized as an impulse response of elastic membrane. This dynamic response has been applied for modeling source rupture process as a unit slip function with ω^2 spectral characteristics. The soil ground model for source-site path has been presented as a multi-layered half-space which consists of some soil layers overlying a semi-infinite random medium. The prediction model of ground motion has been presented by the Green's function of soil ground model and the source rupture process model. The excellent prediction potential of this ground motion model has been verified through a simultaneous simulation test against the observed ground motions at some sites during the 1995 Hyogo-ken Nanbu Earthquake[1)].

[1] Manager, NTT Facilities Inc., Tokyo, Japan, E-mail: dohi@rd.ntt-f.co.jp
[2] Former Professor, Kyoto University, Kyoto, Japan, E-mail: biwa110m@soleil.ocn.ne.jp
[3] Professor, Kansai University, Osaka, Japan, E-mail: asano@ipcku.kansai-u.ac.jp
[4] Lecturer, Kansai University, Osaka, Japan, E-mail: matsuda@ipcku.kansai-u.ac.jp

In this study, to examine precisely the prediction potential of this ground motion model, the attenuation of ground motion with propagation distance has been estimated using the above ground motion model. It has been compared with some observed data at the several sites.

GROUND MOTION MODEL

Source model for rupture process on fault plane

In order to investigate how the source rupture process gives an effect on ground motion, the earthquake source rupture growth process is modeled. This model is presented in terms of seismic moment tensor including the starting and stopping effects of the rupture front at the *m*th fault element, using the above slip vectors and slip function with temporally and spatially random variation due to heterogeneous asperity on the fault surface as follows[1];

$$M_{(m)pq}(\omega) = R_{pq} M_{0(m)} \sum_{j=1}^{N1} \sum_{k=1}^{N2} \frac{\delta_j \gamma_k}{\omega\sqrt{(\omega\Delta\tau_k)^2+1}} \frac{\sin(\omega\Delta T_j/2)}{\omega\Delta T_j/2} \times \exp\left[-i\left\{\omega\tilde{t}_j + \omega\tau_k + \tan^{-1}(\omega\Delta\tau_k) + \pi/2\right\}\right] \tag{1}$$

$$\tilde{t}_j = \sum_{l=1}^{j-1} \Delta T_l + \Delta T_j/2, \quad \tau_k = \sum_{l=1}^{k-1} \Delta\tau_l, \quad M_{0(m)} = \mu\Delta u'_{(m)} L_{(e)} W_{(e)}$$

where $M_0(m)$, $\Delta u'_{(m)}$, R_{pq} and μ are seismic moment, average slip displacement, radiation pattern and shear rigidity at the *m*th fault element, and ΔT_j and $\Delta\tau_k$ are the fluctuating rupture time and rise time due to the small-scale heterogeneity on the fault plane, ω is the frequency, N_1 and N_2 denote the event number and the fluctuating number associated with building up dislocation at the *m*th fault element. δ_j and γ_k are the weighting factors for the dislocation amplitude. $\{\delta_j\}$, $\{\gamma_k\}$, $\{\Delta T_j\}$ and $\{\Delta\tau_k\}$ in Equation (1) are considered random variables with a uniform distribution, the coefficients of variation of which are taken to be 0.2. N_1 and N_2 in Equation (1) are set to be 5 so that the source model includes the maximum frequency component of up to 10 Hz by producing a short fluctuating rise time $\Delta\tau_k$.

For the reference case of this study, the source rupture process of an earthquake of Magnitude M=7.7 is modeled for a rectangular fault plane with length L=100 km and width W=50 km placed in a semi-infinite homogeneous region as shown in Figure 1. The fault plane is fixed with strike direction angle 0^o and dip direction angle 45^o. The rake angle is 0^o.

The seismic moment of the earthquake is $M_0 = 6.31\text{x}10^{27}$dyne•cm. The fault plane is divided into N_w x N_L =10 x 20 subfaults with equal area $\Sigma_{(m)} = \Sigma_e = L_e$ x W_e as shown in Figure 1. The total seismic moment is distributed on each subfault in proportional to the random numbers δ_j. The average slip over the entire fault plane is 281cm. In this study, the seismic moment distribution is supposed as shown in Figure 2. The source rupture initiates at the left (south) side area of the fault plane, propagates laterally along the fault length with a random velocity with average 3km/s and arrives at the right (north) side of the fault plane. The seismic moment is assumed to be released at the every time when the source rupture front arrives at the center point on each fault element.

This source rupture growth process on the entire fault plane may be modeled as the sum of elementary seismic moments releasing with the random lagged times $t_r(\xi_{(m)})$ to the rupture events on the fault surface. Then the source spectra of the large event is shown to be

$$S_0(\omega) = \left| \sum_{j=1}^{N} \dot{M}_{0(m)}(\omega) \exp\left[-\omega\, t_r\left(\xi_{(m)}\right)\right] \right| \tag{2}$$

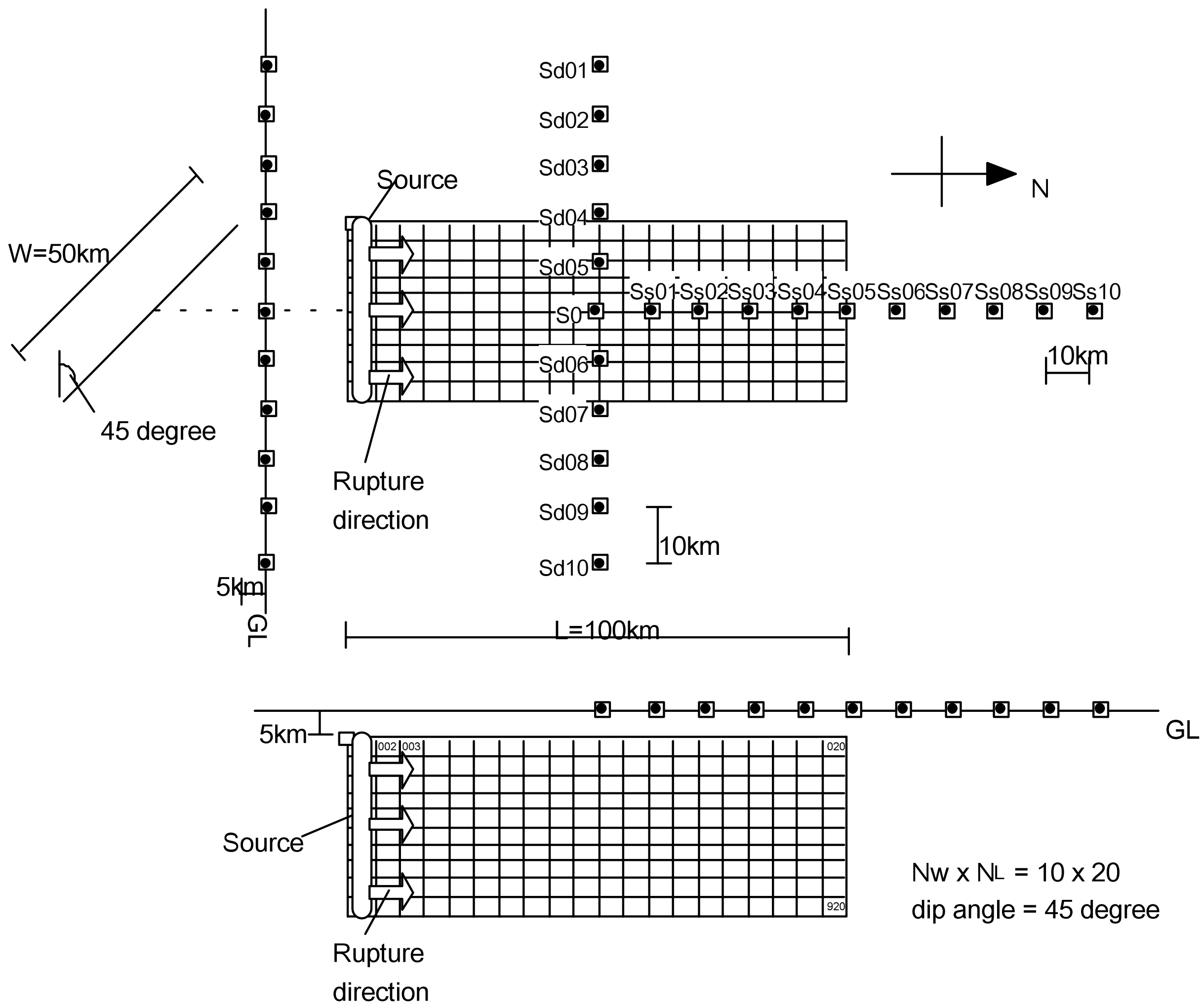

Figure 1 Fault plane, source rupture initiation area on the left side of fault plane, source rupture direction, and observation sites on the Ss- and Sd-lines

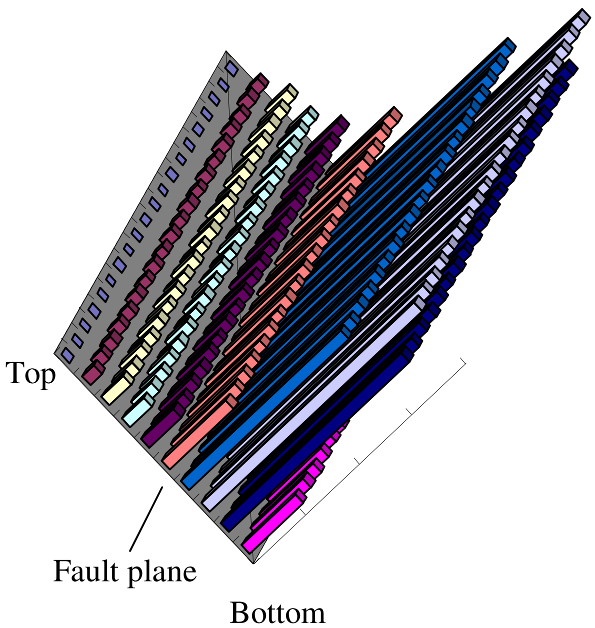

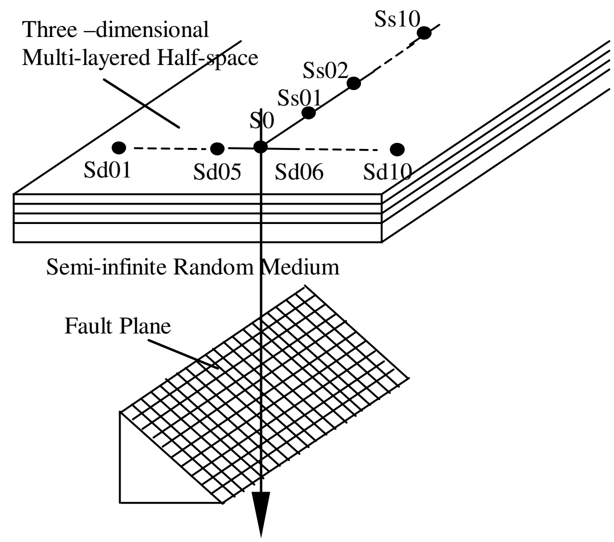

Figure 2 Seismic moment distribution on fault plane

Figure 3 Geometric relation between causative fault and observation sites

Soil sediment structure model for source-site path

The direct waves from source area and their first reflection waves are considered to be most reliable waves for seismic design of a structural system. In this study, the ground motion model will consider the problem in essential way by taking into account the two representative physical phenomena; the scattering of seismic waves in the lithosphere region and the amplification of seismic waves in surface soil sediment structure over the lithosphere region. Then the refined soil sediment structure model for source-site path could be presented as a multi-layered half-space which consists of a surface layer overlying a semi-infinite random medium.

Ground motion model

The ground motion consists of wave motions with the rupture events occurring at the 200 subfaults of a rectangular fault plane in a semi-infinite homogeneous medium as shown in Figure 3. When $\Delta u_{(m)}(\xi,t)$ takes place at the center point $\xi_{(m)}$ located on a subfault $\Sigma_{(m)}$, the *n*th component of displacement $u_{(m)n}(\mathbf{x};t)$ at observation point x and time t may be represented by the convolution integral as

$$u_{(m)n}(\mathbf{x},t) = M_{(m)pq}(t)\frac{\partial}{\partial \xi_q} G_{np}(\mathbf{x},t;\xi_{(m)},0) \tag{3}$$

where $G_{np}(\mathbf{x}, t ; \xi_{(m)}, 0)$ presents the Green's function of the *n*th component of displacement at the position at x and time t when the unit impulse is applied in the *p* direction at the center point $\xi_{(m)}$ located on the *m*th fault element and time t=0. $M_{(m)pq}(t)$ is described by the source rupture process model. Then the ground motion may be expressed by the summation of seismic waves radiated from all the rupture events on the entire fault plane as

$$u_n(\mathbf{x}, t) = \sum_{m=1}^{N} u_{(m)n}(\mathbf{x};\ t - t_r(\xi_{(m)})) \tag{4}$$

in which $\xi_{(m)}$ and $t_r(\xi_{(m)})$ are the center point and dislocation initiation time on the *m*th fault element $\Sigma_{(m)}$. In this ground motion modeling, the source directivity effects could be realized by the two time differences with wave propagation; the one is the arriving time difference at the site on the two wave motions radiated from the starting and stopping phases; the other is the traveling time difference at the site on wave motions radiated from the different subfault on the fault plane. Then such directivity effects could be produced with the surface integration of wave motions over the entire fault plane, which are expressed by the convolution of Green's function and source model reflecting the irregular rupture process on the entire fault plane.

NUMERICAL EXAMPLE

The ground motions calculated by Equations (3) and (4) are shown for the one soil sediment structure model at the 21 observation sites under the fault-site geometry relation in Figure 1. The site S0 is situated just above the center of fault plane. The sites Sd01, Sd02, … , Sd10 and the Ss01, Ss02, …., Ss10 are located in the dip direction on the fault plane (EW direction), and in the strike direction on the fault plane (NS direction), respectively. The same soil sediment structure model in Table 1 is supposed for all the sites. The amplification factors of this soil sediment structure model are shown in Figure 4.
The large components are recognized in the short period range about 0.2 and 0.4 sec. They reflected the amplification characteristics of shallow surface soil sediment layers. Some large components are also clearly recognized in the long period about 2, 5, and 10 sec. They correspond with the predominant periods of deeper soil sediment layers.

Wave form function and response spectra

Figures 5 and 6 show acceleration time histories and velocity response spectra with 5% damping ratio for NS, EW and UD components of ground motions at the observation sites Sd(i) (i=1~10) on the center line of fault plane.

Table 1 Soil sediment structure model

Depth H(m)	P-wave velocity Vp(m/sec)	S-wave velocity Vs(m/sec)	Density ρ(g/cm3)	Damping factor h(%) Vp	Damping factor h(%) Vs
0-3.45	1,450	220	1.70	1.0	1.0
3.45-8.35	1,450	220	1.60	1.0	1.0
8.35-23.15	1,870	540	1.75	1.0	1.0
23.15-29.8	1,810	520	1.80	1.0	1.0
29.8-40.2	1,960	570	1.80	1.0	1.0
40.2-85.2	1,800	550	1.90	1.0	1.0
85.2-153	1,800	610	1.90	1.0	1.0
153-1000	1,860	720	1.90	1.0	1.0
1000-3500	2,800	1,500	2.20	0.5	0.5
3500-6000	4,700	2,500	2.40	0.5	0.5
6000-	5,500	3,000	2.50	0.5	0.5

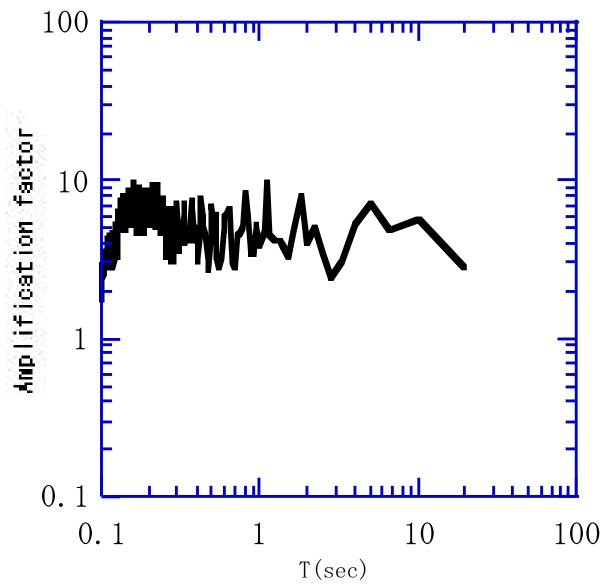

Figure 4 Amplification factors for all the sites

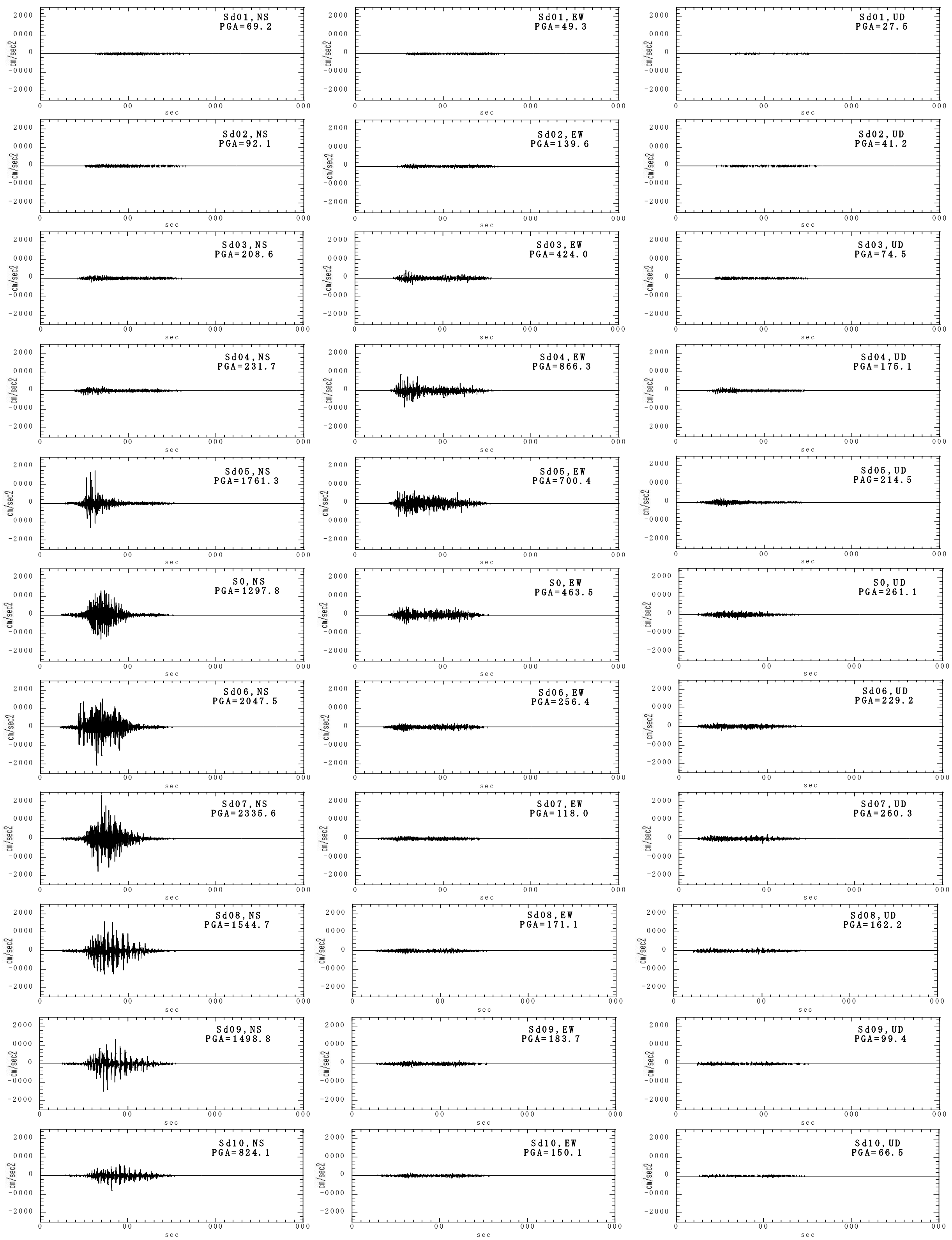

Figure 5-1 Acceleration time histories for NS, EW and UD components of ground motions at S0, Sd01, Sd02, ….and Sd10 sites

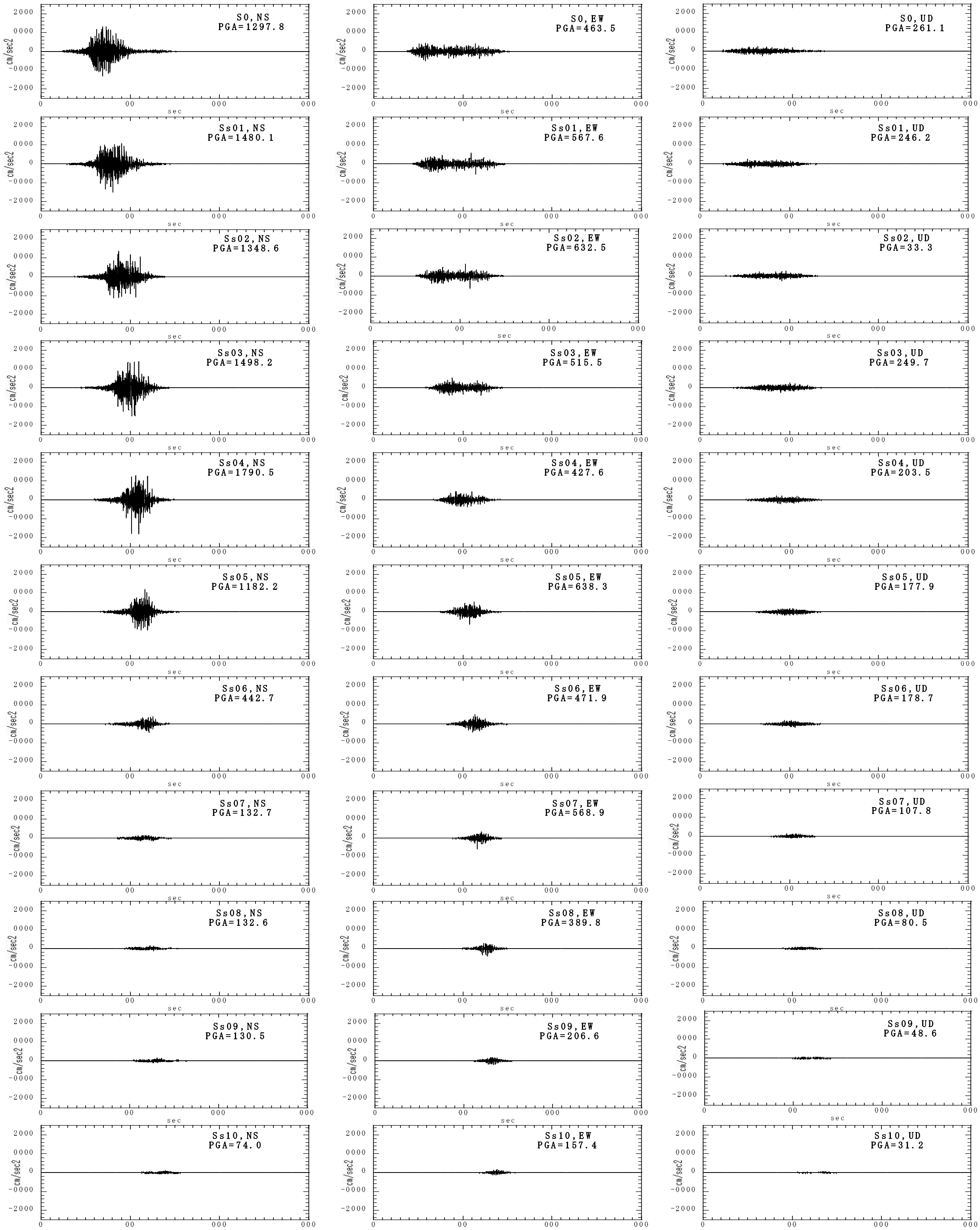

Figure 5-2 Acceleration time histories for NS, EW and UD components of ground motions at S0, Ss01, Ss02, ….and Ss10 sites

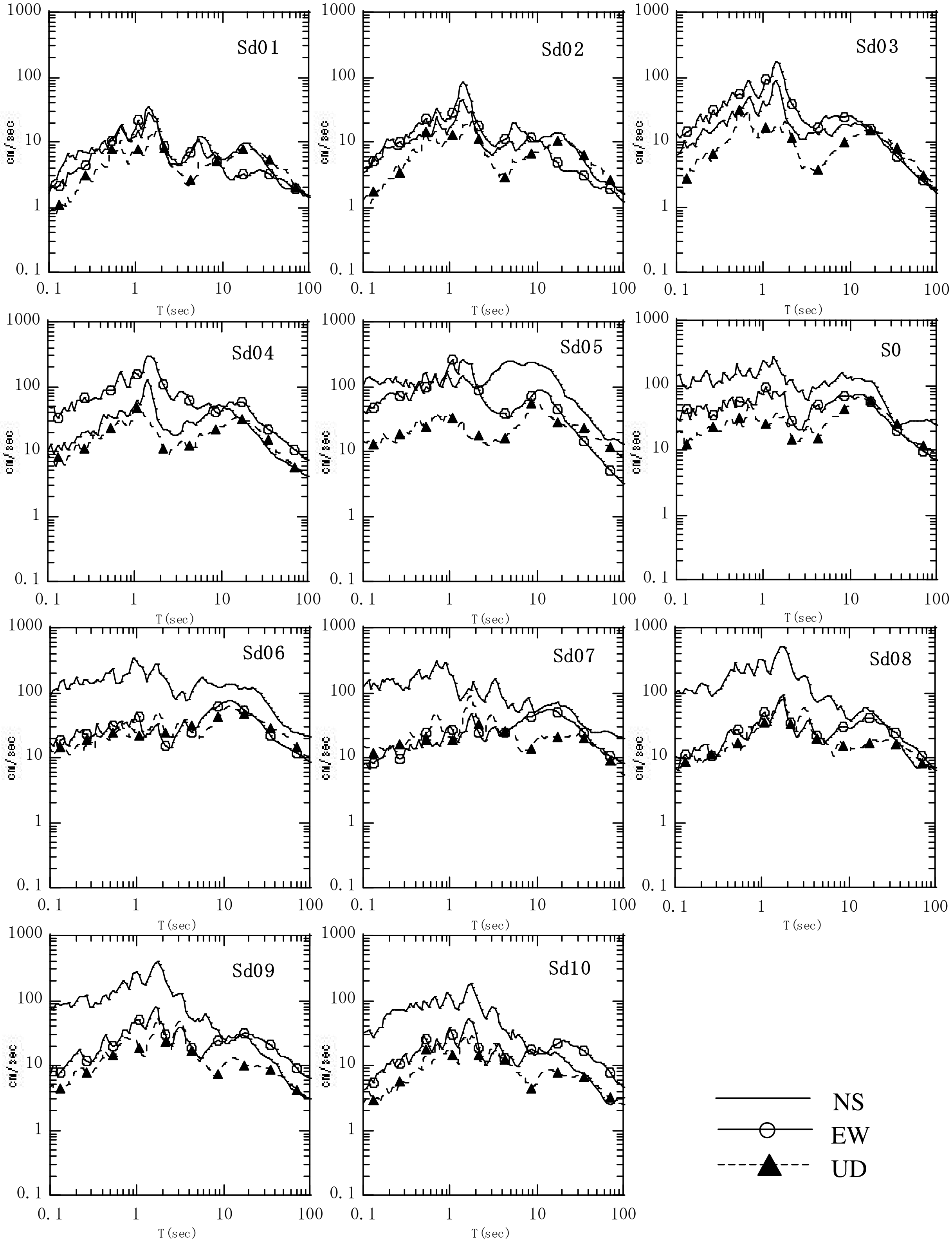

Figure 6-1 Velocity response spectra with 5% damping ratio for NS, EW and UD components of ground motions at S0, Sd01, Sd02, …., and Sd10 sites

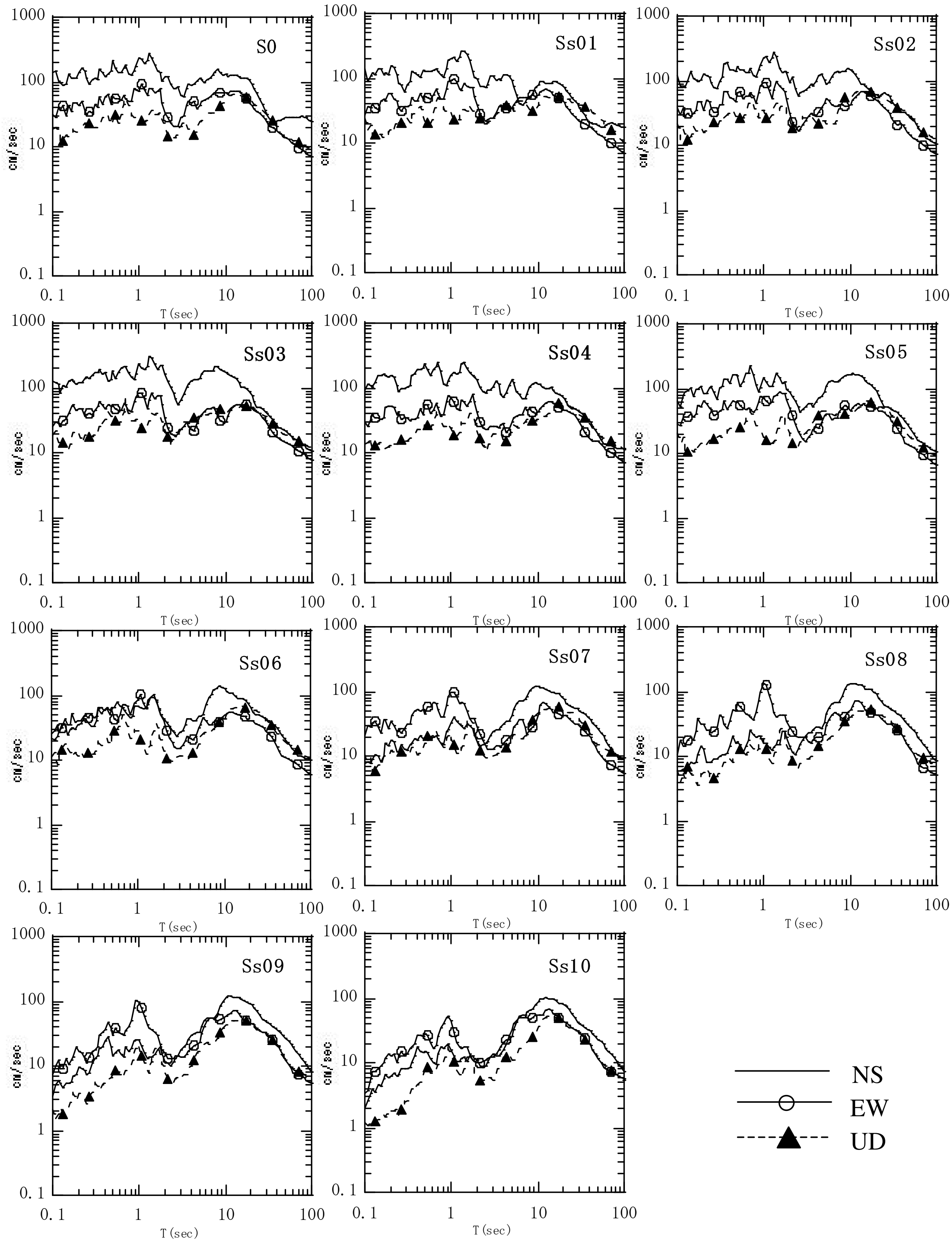

Figure 6-2 Velocity response spectra with 5% damping ratio for NS, EW and UD components of ground motions at S0, Ss01, Ss02, …., and Ss10 sites

Attenuation curves

Figures 7 and 8 show acceleration and velocity attenuation relationship in distance for ground motions at all the sites. The focal distance is supposed to be the shortest distance from fault plane to each site.
There is clear difference in the attenuation relationships between the sites Sd01, Sd02, Sd03, Sd04 located at the upper side of center line cross the fault length direction and the sites Sd06, Sd07, Sd08, Sd09, Sd10 located at the lower side of center line cross the fault length direction. The maximum acceleration and velocity values of ground motions at the sites Sd01, Sd02, Sd03, Sd04 are larger than those of the sites Sd06, Sd07, Sd08, Sd09, Sd10.

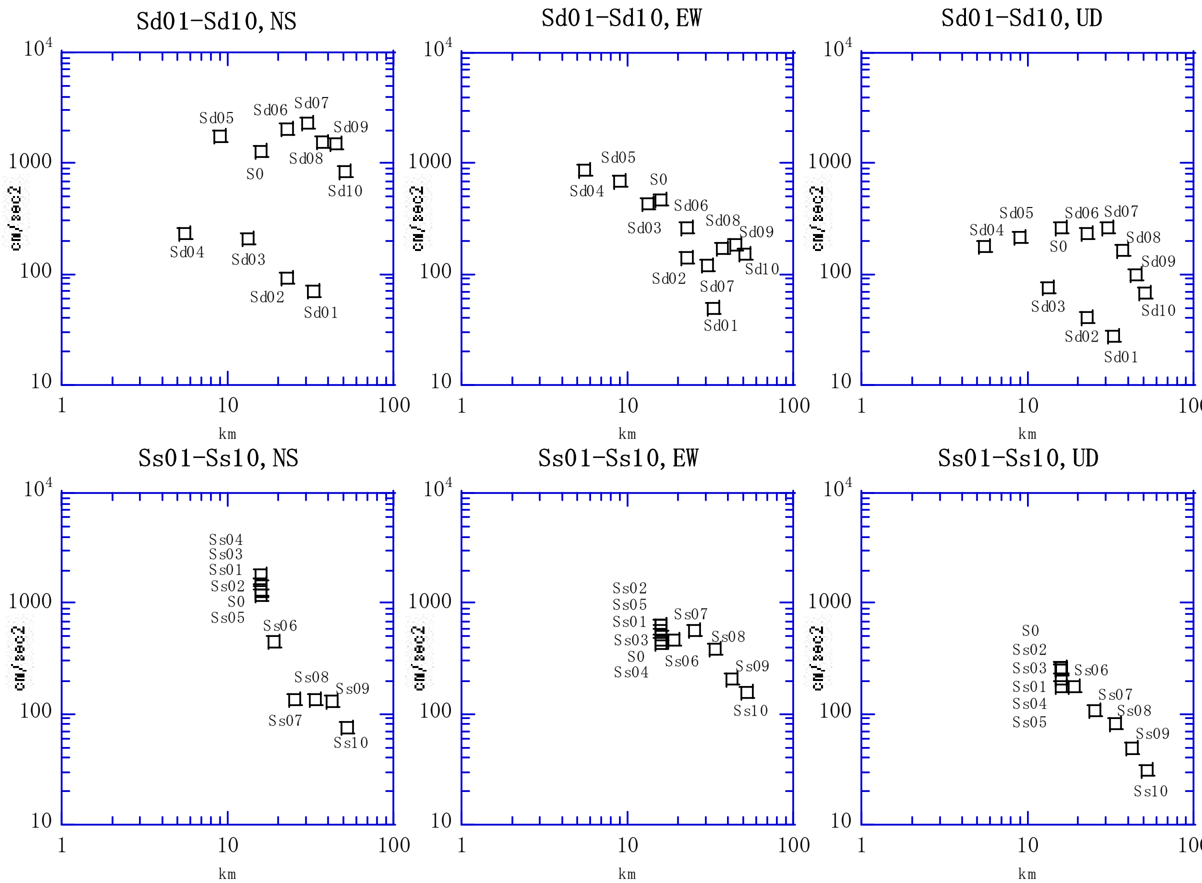

Figure 7 Attenuation of acceleration ground motions in distance along the Sd- and Ss- line sites on the fault plane

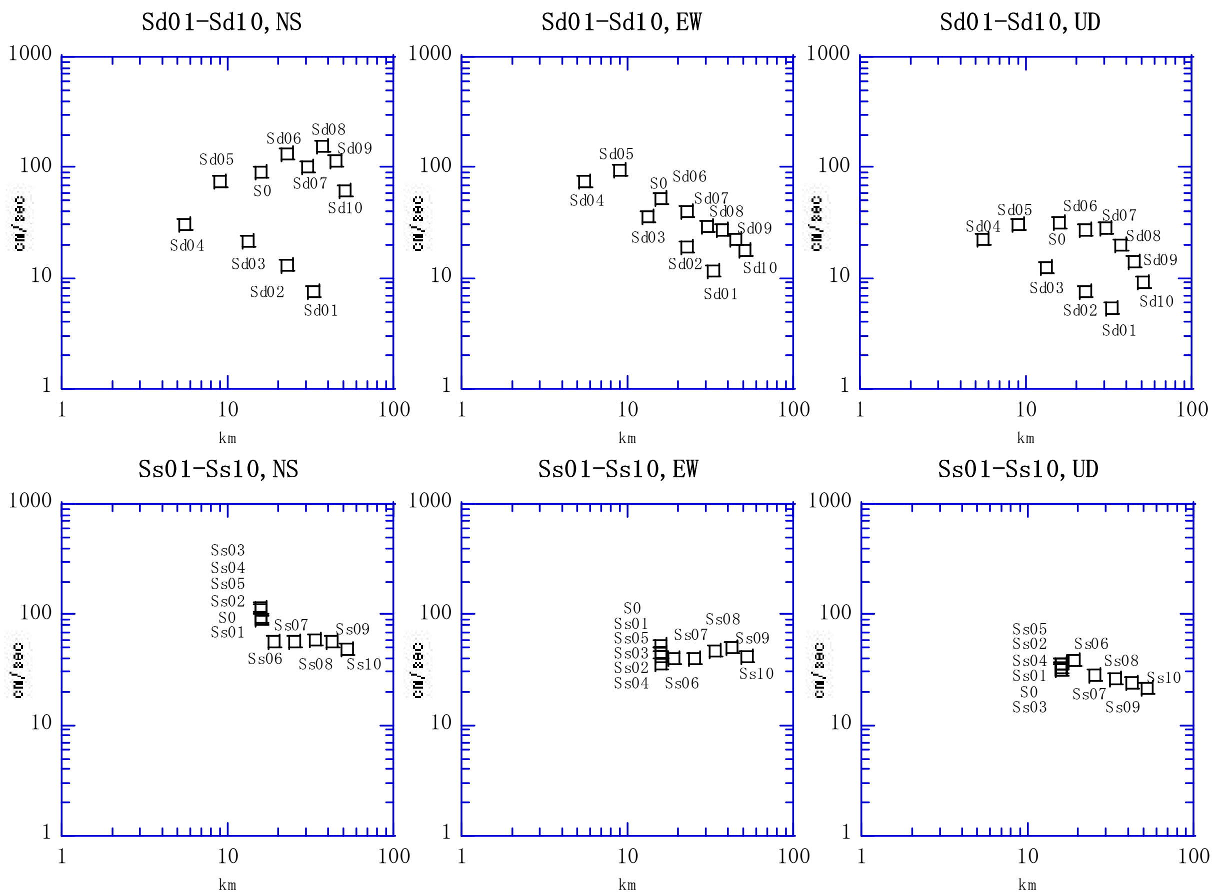

Figure 8 Attenuation of velocity ground motions in distance along Sd- and Ss- line sites on the fault plane

CONCLUSIONS

In this study, the ground motion model has been applied to predict the attenuation of peak values and response spectra of the ground motions with propagation distance. The investigation results have suggested that the accurate prediction of ground motion depends on the derivation of the physical laws and quantities which could describe essentially the characteristics of ground motion. They are the source-site geometry, particularly the ratio of epicentral distance to focal depth, the source-site distance, and the directivity effects in the source radiation.

REFERENCES

1. Kawano M, Dohi H, Matsuda S. Verification of Predicted Non-linear Site Response during the 1995 Hyogo-Ken Nanbu earthquake. SDEE, 2000; 20: 493-507.
2. Fukushima Y, Tanaka T. A New Attenuation Relation for Peak Horizontal Acceleration of Strong Earthquake Ground Motion in Japan. BSSA, 1999; 80, 4: 757-783.
3. Vladislav G. Martynov, Frank L. Vernon, Robert J. Mellors, and Gary L. Pavlis. High-frequency Attenuation in the Crust and Upper Mantle of the Northern Tien Shan. BSSA, 1999;89, 1:215-238.
4. Boore M. D, Smith E. C. Analysis of Earthquake Recordings Obtained from the Seafloor Earthquake Measurement System (SFEMS) Instruments Deploy of the Coast of Southern California. BSSA, 1999;89, 1:260-274.